Chemical Science

ROYAL SOCIETY OF CHEMISTRY

PERSPECTIVE

View Article Online
View Journal | View Issue

Cite this: *Chem. Sci.*, 2020, **11**, 1728

All publication charges for this article have been paid for by the Royal Society of Chemistry

Received 18th December 2019
Accepted 23rd January 2020

DOI: 10.1039/c9sc06418d

rsc.li/chemical-science

Bioinspired chemistry at MOF secondary building units

James R. Bour, † Ashley M. Wright, † Xin He and Mircea Dincă *

The secondary building units (SBUs) in metal–organic frameworks (MOFs) support metal ions in well-defined and site-isolated coordination environments with ligand fields similar to those found in metalloenzymes. This burgeoning class of materials has accordingly been recognized as an attractive platform for metalloenzyme active site mimicry and biomimetic catalysis. Early progress in this area was slowed by challenges such as a limited range of hydrolytic stability and a relatively poor diversity of redox-active metals that could be incorporated into SBUs. However, recent progress with water-stable MOFs and the development of more sophisticated synthetic routes such as postsynthetic cation exchange have largely addressed these challenges. MOF SBUs are being leveraged to interrogate traditionally unstable intermediates and catalytic processes involving small gaseous molecules. This perspective describes recent advances in the use of metal centers within SBUs for biomimetic chemistry and discusses key future developments in this area.

Biomimetic chemistries in crystalline porous materials

Chemists have long sought to understand and emulate the remarkable chemical reactions catalyzed by metalloenzymes. Synthetic biomimetic inorganic chemistry aims to understand enzymatic function through the creation of structural and functional models of active sites.[1] Through replication of the active site in synthetic systems (molecular & solid-state), scientists aim to achieve metalloenzyme function without the limitations of natural enzymes. To date, most biomimetic inorganic chemistry has been studied with solution phase model complexes. The power of this strategy is rooted in the highly tunable ligand fields enabled through organic synthesis and interrogated through solution phase spectroscopies (*e.g.* nuclear magnetic resonance). More recently, however, porous crystalline solids such as zeolites and mesoporous silicas have emerged as complementary platforms for the study of biomimetic inorganic chemistry.[2]

Several important parallels exist between metalloenzymes and metal sites in permanently porous crystalline materials. For instance, the restricted translation or complete immobilization of metal centers in these materials is expected to limit or completely inhibit interactions between metals. This property mimics the shielding effect of the large peptide support in metalloenzymes. Indeed, the enormous bulk of the protein often provides local steric and extended spatial protection of the active site thereby reducing its interactions with other metals. The extended three-dimensional structure of the protein protects the active site and modulates active site accessibility through steric or polarity gating of substrates, thereby enforcing product selectivity. With careful material choice and design, the solid-state structures of porous solids can simulate the reactivity and selectivity resulting from the greater steric and polar environment of the metalloenzyme.[3]

Although differences between metalloenzymes and porous solid supported metals can present notable challenges and limitations, such disparities can also engender new analytical and synthetic approaches.[2] For example, porous materials can support highly coordinatively unsaturated metals that are difficult to produce in solution phase. Furthermore, spectroscopic studies of reactive intermediates and biologically relevant gaseous small molecules on solid-supported metals can be performed without the interference of solvent. Permanent porosity also enables the use of reaction media in which traditional model complexes may exhibit limited solubility, stability, or other unfavorable interactions. Finally, solid-supported metals are often more stable than the metalloproteins they emulate and may thus be compatible with harsher or more convenient reagents. In other words, unnatural reactants can be used to generate the key biologically inspired active species (*e.g.* accessing [Fe(IV)=O] with N_2O), which lends these materials to potentially robust catalytic applications.

Despite the numerous opportunities for porous solids in bioinspired chemistries, this promising area of research has arguably lagged behind advances made in other applications of crystalline porous solids such as gas separations, gas storage, and catalysis. Precise knowledge of ligand sphere and tunable

Department of Chemistry, Massachusetts Institute of Technology, 77 Massachusetts Avenue, Cambridge, Massachusetts 02139, USA. E-mail: mdinca@mit.edu

† These authors contributed equally.

ligand properties has proven important in the realization and rationalization of bio-relevant reactivity of molecular models. Corresponding characterization and controlled manipulation of the ligand sphere of solid-supported metals (*e.g.* zeolites, mesoporous silicas, *etc.*) is comparatively difficult.[2,4] Moreover, even modest tuning of secondary sphere interactions remains a considerable challenge in most porous solids.

Metal–organic frameworks (MOFs) stand out among microporous solids because they are atomically and periodically precise, much like zeolites in this sense. Unlike zeolites or other porous solids, MOFs span a broad compositional space that covers essentially the entire periodic table and provides unparalleled chemical and structural tunability. As such, they hold substantial potential to address the long-standing challenges of biomimetic chemistries in the solid state.[5,6]

A variety of different strategies are amenable for incorporating biomimetic metal active sites into MOFs. These approaches include metallolinkers,[7] non-covalent encapsulation of molecular compounds and enzymes,[8,9] templated metal/ligand assemblies,[10] and the use of the metal ions or clusters comprising the secondary building units (SBUs). This perspective describes recent developments and future directions in bioinorganic chemistry and biomimetic catalysis centered at metal–organic framework SBUs. Our contribution is not intended to be comprehensive. Rather, we focus on recent advances that highlight the unique properties of SBU-based metals in their reactions with biologically important gaseous molecules (*e.g.* NO, CO_2, *etc.*). Accordingly, we do not discuss bioinspired chemistry centered primarily at the organic linker, MOF-enzyme composites, or molecular species encapsulated in MOF pores. These are conceptually distinct approaches that have been extensively reviewed elsewhere.[9,11–15]

SBU-based biomimetic chemistry

Metal ions comprising the SBUs share many structural and electronic characteristics with the active sites of metalloenzymes (Fig. 1). They are site-isolated and are typically coordinated to the organic linker by carboxylate, azolate, imidazolate, phenolate, or thiolate donors. These functionalities are similar, or in some cases, identical to the carboxylate, histidine, thiolate, or phenolate moieties that often form the coordination sphere of active sites in metalloenzymes. These weak field ligands commonly result in high-spin electronic configurations, again similar to those found in metalloenzymes. Although the similarity between MOF SBUs and enzyme active sites has long been recognized, the use of SBUs for inner-sphere small molecule chemistry is a relatively recent development. Practical challenges associated with hydrolytic stability and incorporation of redox active ions at the SBU has historically impeded progress in this area.[16] Many of these obstacles have now been overcome through better understanding of the kinetic stabilization of MOF structures.[76] Furthermore, a wide variety of effective synthetic methods for control of the SBU primary structure and secondary structure properties now enable robust bioinspired chemistries in MOFs.

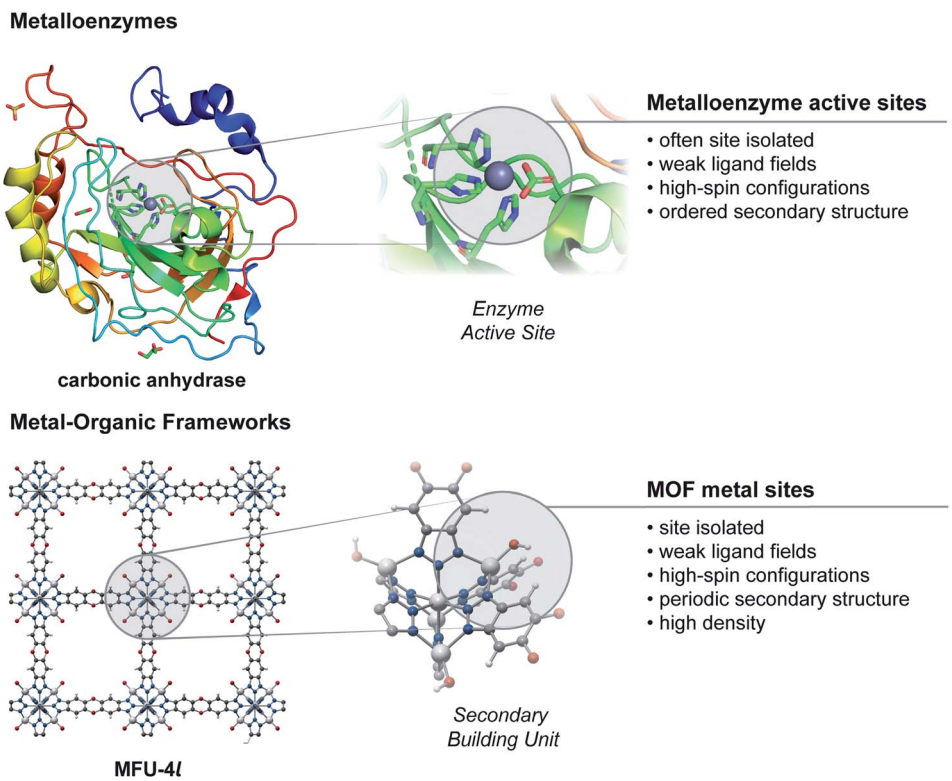

Fig. 1 Comparison of properties between metalloenzyme actives sites and metal sites in metal–organic frameworks.

Synthetic approaches to control primary structure

Incorporation of biologically relevant transition metal ions into MOF SBU is generally achieved through one of three strategies: direct synthesis, post-synthetic cation exchange, and post-synthetic deposition/grafting on the SBU (Fig. 2). Direct syntheses are a synthetic regime in which the metal ion is present during the synthesis of the material, usually through solvothermal reaction between a common metal salt and free organic linker. This strategy is step efficient and generally leads to high metal content of the desired ion. However, this approach is fundamentally limited by the deterministic reaction and crystallization profiles for a given metal/linker combination. Finely balanced kinetic criteria must often be met for crystallization of the material and synthetic conditions to satisfy these criteria are difficult to determine *a priori*. Direct synthetic methods generally require extensive condition screening. Most limiting is the fact that direct synthesis gives rise to SBUs preferred by the metal/ligand combination. These characteristic SBUs rarely possess the desired metal or oxidation state for a targeted application in small molecule reactivity. One strategy that circumvents the reliance on labor-intensive and structurally inflexible direct synthesis methods is the post-synthetic exchange of metal ions into pre-formed SBUs. Termed cation exchange, this strategy enables the integration of metals into SBUs that cannot be formed by the same metals *via* direct synthesis. Practically, a parent material with the desired SBU is self-assembled from a "sacrificial" parent metal ion, which is subsequently exchanged by the chemically functional metal ion either partially or completely, with retention of the parent SBU and MOF structure.[17] First discovered serendipitously in a systematic study of MOFs used for hydrogen storage,[18] this cation exchange strategy proved to be applicable across a wide variety of MOFs, including notoriously dynamic materials such as MOF-5. Cation exchange generally only refers to instances where a parent metal ion that is part of an SBU is swapped post-synthetically. Other strategies involving exchange of ionically paired cations or grafting of cations on the SBU have also been pursued.[19,20] Although post-synthetic grafting of heterometals on the SBU is operationally simple and widely compatible with numerous materials, it can result in less well-defined coordination environments and therefore does not benefit from the structural fidelity enabled by SBU cation exchange. Nevertheless, taken together, these strategies enable the site isolation of a wide variety of metal ions within or on MOF SBUs.

An additional key component of the SBU primary structure is the non-structural ligands of the material, typically simple hard anions (OH^-, Cl^-, OAc^-) or solvent molecules (DMF, water, *etc.*). These ligands are also incorporated directly during the material synthesis but can sometimes be replaced *via* post-synthetic exchange. Post-synthetic ligand exchanges of non-structural anions or solvent ligands represent a modular way to tune the electronic structure and reactivity of a metal site of interest.[21] Modulation of framework properties through variation of non-structural ligands has already been used to finely tune the adsorption properties of MOFs and has recently been used to enable new bioinspired reactivities at MOF SBUs.[22,23]

Synthetic approaches to control secondary structure

Although it is currently not widely used in the context of biomimetic chemistry, changing the secondary structural properties of the MOF through substitution on the organic linker can directly impact the reaction outcome and selectivity.[24] One potential benefit of using MOFs to functionally mimic metalloenzymes is the control over environmental components such as hydrophilicity. Modulation of the secondary structural properties through variation of the organic linker is, in principle, only limited by the organic chemistry needed to make the desired linker and the linker's compatibility with crystallization. However, systematic structure–function

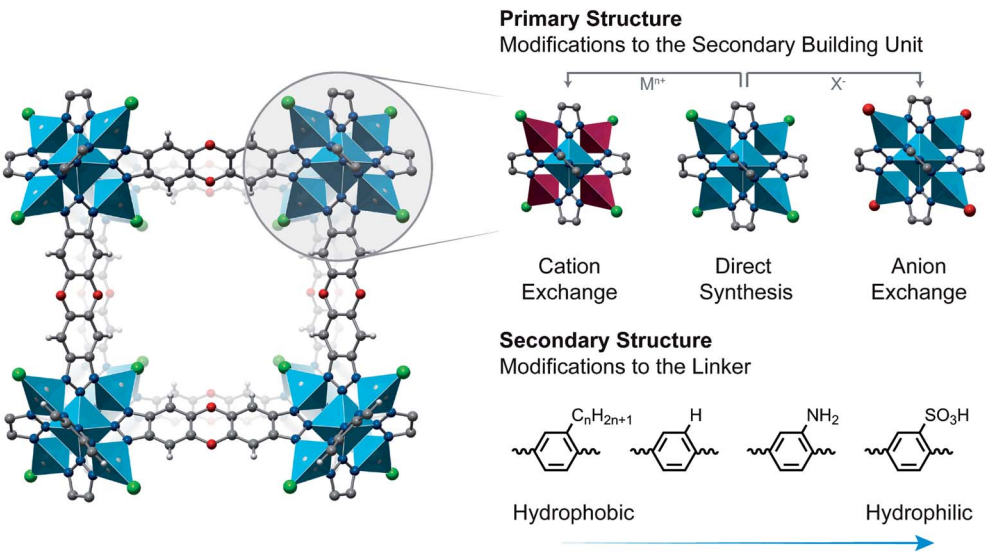

Fig. 2 Modification of the MOF primary structure and secondary structure.

relationship studies on linker functionality are highly labor intensive; minor linker substitutions can prevent or enhance MOF crystallization.[25] Post-synthetic modifications have been developed as an alternative strategy to direct syntheses. For sufficiently labile linkers, treatment of the MOF with a new linker can result in linker exchange with preserved structural integrity.[26] In a separate strategy, reactive handles on a linker (such as NH_2) and the metal node can be systematically functionalized after MOF synthesis.[27] This approach can be highly effective for late-stage derivatization but is itself limited by the nature of the reactive handle and its compatibility with MOF synthesis.

Chemistry of bioactive small molecules at MOF SBUs

Here, we highlight examples of biomimetic small molecule chemistry at the SBU.

Carbon dioxide

A bioinspired strategy for the capture of CO_2 is being explored as an alternative approach to conventional amine-based absorption materials such as liquid amines or alcohols.[28] Carbonic anhydrases (CA) are a family of metalloenzymes that catalyze the hydration and dehydration of carbon dioxide ($H_2O + CO_2 \rightleftharpoons HCO_3^- + H^+$).[29] The critical elementary step in this transformation is the reaction of a terminal nucleophilic metal hydroxide, typically a zinc hydroxide in a $N_{(His)3}ZnOH$ coordination environment, with CO_2. The reversibility of insertion of CO_2 into the metal–hydroxide bond makes Zn–OH moieties an attractive target for energy efficient capture of CO_2 and subsequent release.

MOFs have long been studied as adsorbent materials for CO_2 capture.[30,31] Conventional strategies include physisorption, reaction with appended amines, and encapsulation of molecular catalysts.[32] Using bioinspired chemistry at the SBU, Zhang and co-workers installed terminal hydroxide groups by reacting hydrogen peroxide with redox active metals in $M^{II}_2Cl_2(bbta)$ (M = Mn, Co; H_2bbta = 1*H*,5*H*-benzo(1,2-*d*:4,5-*d*′)bistriazole).[33] Inclusion of the terminal hydroxide in the partial oxidation product, $M^{II}M^{III}(OH)Cl_2(bbta)$, augments CO_2 sorption capacities by a factor of 4 or 5 over the parent $M^{II}_2Cl_2(bbta)$ materials at low pressures (0.15 bar). Infrared (IR) spectroscopic analysis of the CO_2-loaded material revealed formation of a bicarbonate moiety similar to the first step in CA chemistry. Notably, the material adsorbs CO_2 even in high relative humidity (RH = 82%) conditions, an improvement over physisorption materials. Although $M^{II}M^{III}(OH)Cl_2(bbta)$ has similar features that mimic CA, it is not structurally analogous.

In contrast, the triazolate MOFs, $Zn_5(OH)_4(bibta)_3$ (CFA-1-(OH), H_2bibta = 5,5′-bibenzotriazole)[34] and $Zn_5(OH)_4(btdd)$ (MFU-4*l*-(OH), H_2btdd = bis(1,2,3-triazolo[4,5-*b*],[4′,5′-*i*]) dibenzo[1,4]dioxin)[35] feature SBUs that are close structural homologues of the CA active site (Fig. 3). In both materials, SBUs are Kuratowski clusters, which feature a central octahedral zinc(II) with six bridging azolate ligands and four peripheral

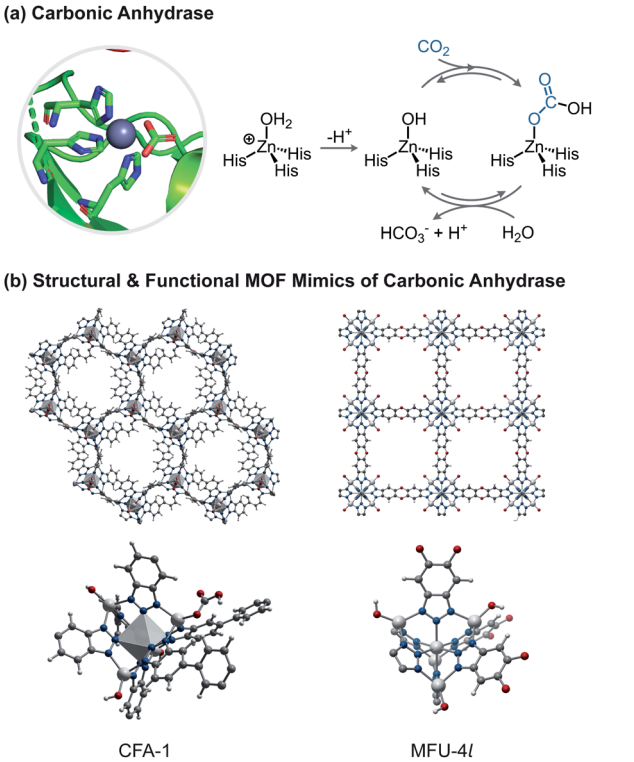

Fig. 3 (a) Depiction of the carbonic anhydrase active site and schematic of the hydration mechanism. (b) DFT optimized structures of CFA-1 (left) and MFU-4*l*-(OH) (right) along with an expanded view of the secondary building unit/metal node.

tetrahedral zinc(II) sites with an exchangeable X-ligand.[36] The peripheral zinc(II) site is structurally and electronically similar to the active site in CA; it features an N_3ZnX coordination environment comprised of three triazolate nitrogen donors, which are electronically similar to histidines. In addition to their structural mimicry, these materials also engage in reactivity that functionally mimics CA. The parent CFA-1 material, $Zn_5(OAc)_4(bibta)$, hydrolyzes *para*-nitrophenyl acetate and CO_2 under basic conditions.[37] In a separate study, CFA-1-(OH) was directly prepared by anion exchange of the acetate ligand in CFA-1 with bicarbonate followed by heating to 100 °C to induce decarboxylation.[22] Sorption studies on CFA-1 and CFA-1-(OH) revealed significant improvement in CO_2 uptake in the hydroxide material. Interestingly, because CFA-1 is a chiral material, the Zn–X sites in the SBU are not all equivalent, and periodic calculations showed that once formed, a bicarbonate may interact with a second Zn–OH group or Zn–CO_3H group at an adjacent SBU representing an unusual example of secondary coordination sphere effects in MOFs. The ensuing hydrogen bonding interaction enhances the initial CO_2 sorption profile.[22]

Exhibiting the same SBUs as CFA-1, MFU-4*l* differs from the former in being a cubic MOF with equally spaced SBUs and N_3ZnX sites (Fig. 3). As with CFA-1, terminal hydroxides can be installed in MFU-4*l* ($Zn_5Cl_4(btdd)_3$) by anion exchange with [^{t}Bu$_4$N][OH].[23] MFU-4*l*-(OH) exhibits enhanced CO_2 sorption over its parent chloride material. Further studies demonstrated that MFU-4*l*-(OH) acts as functional mimic of CA: it catalyzes the

isotopic exchange between $H_2{}^{18}O$ and CO_2 as well as the hydrolysis of *para*-nitrophenyl acetate. Detection of the bicarbonate ligand after reaction with CO_2 by IR spectroscopy suggests that the isotopic exchange mechanism is similar to that in CA, where CO_2 reversibly inserts into the Zn–OH bond.

These CA models highlight important opportunities and limitations of SBU-based model systems. Some of the primary advantages of these systems are the high density and site isolation of the zinc centers, which allow convenient spectroscopic characterization of the CO_2 insertion process without complications arising from bimolecular processes. Solution phase CA models can undergo bimolecular decomposition through the formation of dizinc carbonate products.[38] This undesired reaction is not observed with the native enzyme. Although a high density of metal active sites can facilitate characterization, it also creates challenges. Both MFU-4*l*-(OH) and CFA-1-(OH) possess four accessible Zn–OH motifs per SBU. CO_2 sorption measurements suggest that each Zn–OH unit is not fully electronically isolated from the other Zn centers in the SBU. The first two equivalents of CO_2 insert with a much higher affinity than the second two equivalents. This effect was attributed to an overall reduction in electron density at the remaining Zn–OH sites in the SBU following initial CO_2 insertions. This example serves as a reminder of potential interplay between multiple metal centers at the SBU and that such interactions should be always considered. Nonetheless, CFA-1-(OH) and MFU-4*l*-(OH) provide important insight into the nature of CO_2 insertion into Zn–OH bonds and thus serve as functional mimics of carbonic anhydrase.

Methane & ethane

The functionalization of methane is a critical component in realigning the chemical feedstock landscape from long aliphatic chain feedstocks to gaseous ones.[39] Selective and incomplete oxidation of the strong C–H bonds in methane and ethane is an outstanding objective for the valorization of these new feedstock landscapes. Biology serves as a major inspiration in the development of selective lower alkane oxidation reactions. For instance, particulate (pMMO) and soluble (sMMO) methane monooxygenases catalyze the oxidation of methane to methanol. The wealth of research aimed at understanding and mimicking MMO reactivity has been reviewed elsewhere.[40] Leading structural proposals for the active sites invoke mono or dinuclear copper centers in pMMO, and dinuclear iron sites in sMMO.[41–43] These motifs are found in a variety of Cu/Fe MOF SBUs and have accordingly been investigated for methane/ethane oxidation activity. Other examples of alkane oxidation by abiological metals and/or oxidizing metal species (*e.g.* cobalt superoxos) are not discussed here.

Yaghi and co-workers employed a strategy involving post-synthetic modification of the SBU to position biologically relevant ligands within the pore of MOF-808, a zirconium MOF.[10] The adamantane shaped pore structure of MOF-808 features an SBU with hydroxide, formate and aquo ligands; post-synthetic installation of carboxylate ligands with pendant imidazoles followed by loading with Cu(I) ions under air resulted in bridging dimeric copper(II) species located within the pore.[10] Oxo-bridged copper centers have been proposed (but recently called into question, *vide infra*) as intermediates in the oxidation of methane to methanol by pMMO.[42] Sequential isothermal treatments of 3% N_2O in He followed by flow of CH_4 for one hour at 150 °C resulted in the formation of methanol with productivities ranging from ~1.5–2.5 mmol MeOH per mol Cu dependent on the imidazole ligand (Table 1), with no loss of MOF crystallinity. A Cu_2O_2 active site proposed from density functional theory (DFT) was supported by X-ray absorption spectroscopy. Although precise mechanistic and structural features of this reaction are still unclear, this example represents an important development in the use of the MOF pore structure to template the formation of inorganic assemblies that mimic proposed enzyme active sites.

In an alternative strategy, Lercher and co-workers deposited Cu(II) ions onto the zirconium SBU of NU-1000.[44,45] The modified MOFs outperform the unmodified ones in methane oxidation (Table 1). Activation occurs by exposure to 1 atm of O_2 followed by 1–40 bar methane at 150–200 °C for 0.5 to 3 hours. Attempts to determine the coordination environment of the copper ions using X-ray absorption spectroscopy and DFT revealed multiple trimeric, dimeric, and monomeric copper sites, with the distribution dependent on copper loading: at low Cu loadings mononuclear sites dominate whereas higher Cu loadings give a preponderance of higher nuclearity species. *In situ* structural characterization revealed oxidation state and nuclearity of copper sites remain unchanged during the O_2 treatment. The authors concluded that dinuclear oxyl centers

Table 1 Oxidation of methane catalyzed by MOF-based materials

MOF	Oxidant	Methanol productivity (μmol MeOH per g MOF)	Methanol productivity (mmol MeOH per mol Cu)	Ref.
NU-1000	O_2	0.3		45
Cu-2.9-NU-1000	O_2	4.1	9.7	45
Cu-1.9-NU-1000	O_2	2.0	6.2	45
Cu-0.6-NU-1000	O_2	0.15	1.4	45
MOF-808-His-Cu	N_2O	31.7	~13	10
MOF-808-Iza-Cu	N_2O	61.8	~22	10
MOF-808-Bzz-Cu	N_2O	71.8	~23	10
MIL-53(Al, Fe)	H_2O_2	14 000		46

are the active site for methane oxidation, which is supported by stoichiometric activity, *in situ* structural characterization, and DFT.

In copper-grafted MOF-808 and NU-1000 materials, the preferential designation of the active site is a dimeric Cu(II). Although the pMMO active site was also long thought to feature two or more copper ions,[47] recent studies suggest that it is most likely a mononuclear site.[42] Future studies of monocopper sites at SBUs may provide insight into the nature of such species and should be studied in due course. Overall, these studies complement additional investigations of copper-mediated and catalyzed methane oxidation chemistry within other porous materials.[48–51]

Unlike pMMO, where the nuclearity of the active site is still debated, the hydroxylase subunit of soluble methane monooxygenase (sMMO) is generally agreed to feature a dimeric Fe active site.[40] Suitably spaced diiron motifs have been reported in MOFs and evaluated for oxidase-like activity. Gascon and coworkers recently reported that the controlled incorporation of Fe into MIL-53(Al) results in a catalyst with high selectivity for methane oxidation in the presence of H_2O_2.[46] Preparation of MIL-53(Al, Fe) was most easily controlled using an electrochemical synthetic approach. Fe loadings of 0.3–5.5 wt% with homogeneous distributions were reliably achieved without generation of extraframework Fe species such as Fe_2O_3. Using DFT, the same authors identified key dimeric Fe sites which were best for activating H_2O_2 and oxidizing methane. Critically, MIL-53(Al, Fe) reproduces the key features of sMMO and, unlike molecular models, the rigid MOF structure enforces the dimeric state, thereby limiting decomposition to inactive monomeric species. Furthermore, in contrast to the sensitivity of sMMO enzymes towards H_2O_2, MIL-53(Al, Fe) is stable in the reaction media which facilitates the design of a robust MOF-based catalyst for methane activation.

The compatibility of MIL-53(Al, Fe) with H_2O_2 underscores two important distinctions between biomimetic MOFs and the enzymes they emulate. First, the key active species can be accessed with reagents and conditions that are too harsh for most enzymatic catalysis. Secondly, the high thermal and chemical stability of many MOFs can be exploited to augment the reactivity of biologically inspired intermediates beyond that of the native enzymes. In 2014 Long and coworkers similarly leveraged both of these properties to effect the oxidation of ethane using $Fe_{0.1}Mg_{1.9}$(dobdc), a bimetallic MOF-74 analog. Treatment of this material with N_2O (an oxygen atom transfer reagent) at elevated temperatures resulted in the formation of a reactive intermediate capable of oxidizing ethane.[52,53] DFT calculations implicate a high-spin $S = 2$, Fe(IV)=O species as the active oxidant, which is similar to those proposed for many mononuclear non-heme Fe oxidases.[54,55] In contrast to the diiron active site of sMMO, mononuclear non-heme oxidases are not generally thought to be competent in the oxidation of strong C–H bonds of ethane or methane. The observed oxidation of ethane by the putative Fe(IV)=O species is likely enabled, at least in part, by the high thermal and chemical stability of $Fe_{0.1}Mg_{1.9}$(dobdc).[53]

Oxygen

Dioxygen is a thermodynamically potent oxidant that drives nearly all metabolic processes in aerobic organisms. As a resonance stabilized ground-state triplet, it is kinetically sluggish in the oxidation of singlet substrates.[56] Consequently, most synthetically important transformations involving O_2 activation require enzymes bearing open-shell transition metals such as Fe or Cu.[57,58] Key questions still remain over how these enzymes convert kinetically stable molecular O_2 into strongly oxidizing metal–oxygen species (*e.g.* M–oxo/oxyls, M–hydroperoxos, *etc.*) or how subtle changes in ligand field perturb elementary aspects of O_2 activation. SBU-based Fe and Cu centers provide opportunities to probe detailed features of O_2 activation that underlie some of the most remarkable transformations catalyzed by O_2-dependent oxidases. The permanent porosity and crystallinity of MOFs enable investigation of O_2 binding through gas sorption studies and crystal-to-crystal transformations. This section highlights select examples of O_2 binding and activation at metal sites bearing ligand fields similar to those found in important O_2-activating metalloenzymes.

Some of the earliest steps in studying detailed aspects of O_2 activation with MOFs were reported in 2011 by Long and coworkers, who characterized the temperature-dependent O_2 bonding to the open metal sites in Fe_2(dobdc) (Fe-MOF-74, dobdc^{4-} = 2,5-dioxido-1,4-benzenedicarboxylate).[59] At 298 K, approximately half of the Fe(II) sites bind O_2 irreversibly. Lowering the temperature to 211 K results in reversible O_2 binding and full occupancy of the available Fe(II) sites. The difference in bonding mode at variable temperature was further evidenced by neutron diffraction studies under an O_2 atmosphere at 94 K and 220 K (Fig. 4). At 94 K, partial electron transfer from the Fe^{II} site to O_2 generates $Fe_2(O_2)_2$(dobdc). Warming this material to 220 K results in formal electron transfer from Fe to O_2 to produce a high-spin side-on Fe^{III}–peroxide, as supported by Mössbauer and IR spectroscopy, as

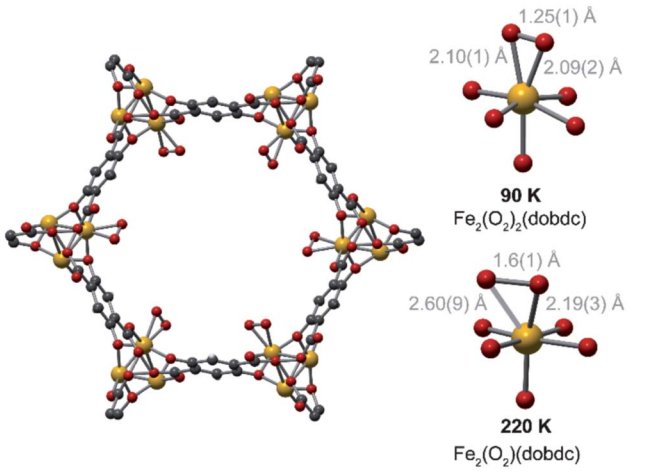

Fig. 4 Depiction of O_2 binding to Fe_2(dobdc) at 90 and 220 K as determined from Rietveld analysis of neutron diffraction data.[59] Orange, grey, and red spheres are Fe, C, and O atoms, respectively.

well as Rietveld refinement of neutron diffraction data. Although this study was originally described in the context of gas separations, these observations are relevant to the chemistry of non-heme diiron oxygenases. The SBU of Fe-MOF-74 enforces a comparable Fe–Fe distance and an all-oxygen ligand field similar to that of oxygenases.[42] The exact nature of O_2 activation in these enzymes is not completely understood.[60] Related studies of O_2 activation by other diiron motifs in MOFs may shed new light on the mechanisms through which diiron oxidases function.

The binding of O_2 to an unsaturated Cu^I center in Cu-exchanged MFU-4*l* has also been probed through sorption isotherm studies.[61] O_2 binds to the unsaturated Cu^I metal site in MFU-4*l* with a heat of adsorption of -53 kJ mol^{-1}. Density functional theory calculations corroborate this value and suggest that O_2 bonds to copper in an end-on rather than side-on (η^2) fashion. Both the energies and geometry of O_2 binding to the Cu(I) sites of MFU-4*l* are in good agreement with thermochemical and structural parameters of solution phase models of monocopper oxidases.[61,62] We also note that determination of bonding enthalpies and coordination modes of O_2 in traditional solution phase model complexes is non-trivial. Competitive formation of dicopper peroxos (Cu–O–O–Cu) or oxidative degradation of the supporting ligand often precludes precise characterization of this elementary step.[63] Such obstacles are not observed in the formation of Cu superoxos in Cu-exchanged MFU-4*l* and are not expected in other site-isolated metal centers of MOFs; additional studies of these systems may yield new fundamental insight into the activation of O_2 by copper-based metalloenzymes.

Nitrogen monoxide

Nitrogen monoxide (NO), also known as nitric oxide, is a highly regulated bio-signaling agent that is crucial for physiological functions such as vasodilation and immune response, and a potent environmental pollutant. Many transformations involving NO require metalloenzymes whose mechanism is not yet completely elucidated.[64] Owing to their inherent site isolation, MOF SBUs are an attractive platform to gain insight into the reactivity of NO by targeting the isolation of reactive intermediates that are difficult to study in the natural systems or in solution. The majority of NO studies with MOFs have focused on NO sorption and on creating NO-releasing materials for therapeutic applications.[65] A variety of MOFs featuring open metal sites, such as, HKUST-1, the MOF-74 (CPO-27) family, and MIL-88(Fe) derivatives, have been explored for the purpose of NO storage and release, but these do not enable further NO reactivity.[66–73]

Of relevance here are reports where NO engages in reactivity mimicking that of metalloenzymes. For instance, cation exchange of Fe(II) into MOF-5 yields Fe-MOF-5 featuring a $FeZn_3O$ cluster in the SBU.[74,75] The Fe(II) ion occupies a pseudo-tetrahedral site and reacts with NO to affect stoichiometric NO disproportionation as evidenced by the formation of nitrous oxide, N_2O, and a Fe(III)–NO_2 group. By monitoring the stoichiometric addition of NO by diffuse reflectance infrared Fourier transform spectroscopy (DRIFTS), Dincă and co-workers were able to identify two intermediates in the reaction mechanism, an iron nitrosyl as well as a radical hyponitrite species ($N_2O_2^{\cdot-}$) (Fig. 5). The latter had not been previously observed spectroscopically and highlights the potential of MOFs as a platform for gaining new insights into complex redox reactivity of small molecules with transition metals. Uniquely to MOFs and their well-defined metal coordination environments, the detection of the intermediate is likely facilitated by site isolation of the Fe(II) site within the MOF structure, which prevents bimetallic reaction pathways.

Importantly, NO disproportionation reactions at Fe centers in MOFs do not occur when the metal coordination sphere is saturated after NO binding, suggesting that at least two open coordination sites are necessary for this reactivity. For instance, Fe-MOF-74, which features a square-pyramidal Fe center with a single open site adsorbs NO strongly to form an iron nitrosyl, as evidenced by the high uptake capacity (6.21 mmol NO per g MOF) at low pressure (0.04 mbar), but does not undergo further reactivity with NO even at a pressure of 7 bar.[70] Fe-MIL-88, also exhibiting a single open coordination site at iron, adsorbs NO to form an iron nitrosyl, but no additional reaction with NO has been reported.[69] The availability of more than one coordinatively unsaturated metal site is thus critical for NO disproportionation and is a feature that is rare in other solids. Taking advantage of multiply unsaturated metal sites in SBUs is a promising avenue for future studies in small molecule reactivity with MOFs.

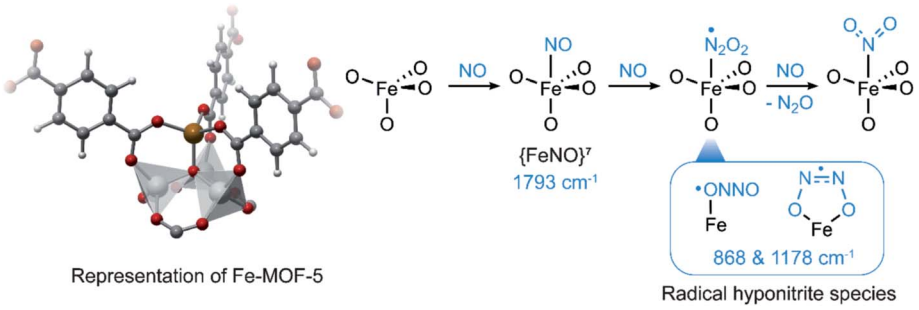

Fig. 5 NO disproportionation at Fe-MOF-5.

Concluding remarks & outlook

In this perspective, we have described developments in the study of bioinspired reactivity at MOF SBUs. When treated as electronically and spatially isolated molecular entities, these become powerful platforms for interrogating small molecule reactivity in an atomically precise, well-defined porous matrix. These studies are the equivalent of matrix-isolation chemistry that is accessible at a wide range of temperatures and without specialized equipment. The ligand fields enabled by the typical MOF ligands are electronically – and sometimes structurally – analogous to those encountered in natural metalloenzymes. Thus, even though enzymes and MOFs are clearly very different classes of chemicals, they share more commonalities: site isolation, ligand fields, electronic structure, open coordination sites, than one would suspect. These unique properties of MOFs are now being leveraged to detect traditionally unstable intermediates and realize functionally biomimetic catalysts. The relatively recent advances made in this area were largely made possible through progress in synthetic methodologies in MOFs over the past 10 years.

We expect future developments in this field to be similarly contingent upon continued advances in the synthesis of readily tunable materials and new MOFs with exchangeable primary structural features and/or multiple open coordination sites. More specifically, the opportunities to affix secondary reaction partners (cofactors) near the SBU is currently underdeveloped in the context of bioinspired chemistries. Current examples of SBU-based biomimetic chemistries are limited to relatively simple systems that are not critically reliant on cooperativity with other motifs. Additional highly tunable materials are needed to realize higher order mimicry of metalloenzymes. Materials featuring functional handles that react in a predictable way with minimal byproducts will enable more advanced mimicry to be realized.

Secondly, discovery of new MOFs with exchangeable primary features (metal cation and non-structural ligands) and multiple unsaturated metal sites will drastically increase the scope of reactivity that can be probed and the number of enzymes that can be functionally mimicked in a stable MOF environment. A large proportion of MOFs feature either inaccessible metals or unexchangeable primary features. MOFs with SBUs featuring unsaturated metal sites, in diverse geometries, and with other pore architectures will significantly improve the breadth of achievable chemistry. These are strong arguments for continued research in fundamentally new MOF topologies and especially new SBU geometries/nuclearities.

With additional suitable materials, improved correlations between the nature of small molecule activation with reactivity can determined. To date, bioinspired chemistries at MOF SBUs have largely focused on either the detailed aspects of small molecule bonding at the SBU or the catalytic reactivity of a material. Fundamental insights that connect elementary bonding with substrate functionalization, catalysis, and mechanism are still rare. We believe that the full potential of this approach will be realized when the unique analytical techniques amenable to MOFs are merged with the catalytic applications of these materials. Such studies will complement existing model platforms to shed new light on the remarkable transformations catalyzed by metalloenzymes and ultimately address outstanding synthetic challenges.

Conflicts of interest

There are no conflicts to declare.

Acknowledgements

We are grateful for support from the National Science Foundation (DMR-1452612) for various fundamental aspects of cation exchange and small molecule chemistry in MOFs. JRB thanks the Arnold and Mabel Beckman Foundation for a Postdoctoral Fellowship.

Notes and references

1 R. H. Holm and E. I. Solomon, *Chem. Rev.*, 2004, **104**, 347–348.
2 B. E. R. Snyder, M. L. Bols, R. A. Schoonheydt, B. F. Sels and E. I. Solomon, *Chem. Rev.*, 2018, **118**, 2718–2768.
3 D. J. Xuereb and R. Raja, *Catal. Sci. Technol.*, 2011, **1**, 517–534.
4 C. Y. Chen and S. I. Zones, *Zeolites Catal.*, 2010, **1**, 155–170.
5 H. Furukawa, K. E. Cordova, M. O'Keeffe and O. M. Yaghi, *Science*, 2013, **341**, 1230444.
6 C. H. Hendon, A. J. Rieth, M. D. Korzyński and M. Dincă, *ACS Cent. Sci.*, 2017, **3**, 554–563.
7 S. M. Cohen, Z. Zhang and J. A. Boissonnault, *Inorg. Chem.*, 2016, **55**, 7281–7290.
8 H. An, M. Li, J. Gao, Z. Zhang, S. Ma and Y. Chen, *Coord. Chem. Rev.*, 2019, **384**, 90–106.
9 R. J. Drout, L. Robison and O. K. Farha, *Coord. Chem. Rev.*, 2019, **381**, 151–160.
10 J. Baek, B. Rungtaweevoranit, X. Pei, M. Park, S. C. Fakra, Y. S. Liu, R. Matheu, S. A. Alshmimri, S. Alshehri, C. A. Trickett, G. A. Somorjai and O. M. Yaghi, *J. Am. Chem. Soc.*, 2018, **140**, 18208–18216.
11 Z.-Y. Gu, J. Park, A. Raiff, Z. Wei and H.-C. Zhou, *ChemCatChem*, 2014, **6**, 67–75.
12 M. Zhao, S. Ou and C.-D. Wu, *Acc. Chem. Res.*, 2014, **47**, 1199–1207.
13 Y. Chen and S. Ma, *Dalton Trans.*, 2016, **45**, 9744–9753.
14 I. Nath, J. Chakraborty and F. Verpoort, *Chem. Soc. Rev.*, 2016, **45**, 4127–4170.
15 K. Chen and C.-D. Wu, *Coord. Chem. Rev.*, 2019, **378**, 445–465.
16 S. Yuan, L. Feng, K. Wang, J. Pang, M. Bosch, C. Lollar, Y. Sun, J. Qin, X. Yang, P. Zhang, Q. Wang, L. Zou, Y. Zhang, L. Zhang, Y. Fang, J. Li and H. C. Zhou, *Adv. Mater.*, 2018, **1704303**, 1–35.
17 C. K. Brozek and M. Dincă, *Chem. Soc. Rev.*, 2014, **43**, 5456–5467.

18 M. Dincă and J. R. Long, *J. Am. Chem. Soc.*, 2007, **129**, 11172–11176.
19 D. T. Genna, A. G. Wong-Foy, A. J. Matzger and M. S. Sanford, *J. Am. Chem. Soc.*, 2013, **135**, 10586–10589.
20 M. J. Hardie, *Encycl. Inorg. Bioinorg. Chem.*, 2014, 1–19.
21 A. J. Rieth, A. M. Wright, G. Skorupskii, J. L. Mancuso, C. H. Hendon and M. Dincă, *J. Am. Chem. Soc.*, 2019, **141**, 13858–13866.
22 C. E. Bien, K. K. Chen, S.-C. Chien, B. R. Reiner, L.-C. Lin, C. R. Wade and W. S. W. Ho, *J. Am. Chem. Soc.*, 2018, **140**, 12662–12666.
23 A. M. Wright, Z. Wu, G. Zhang, J. L. Mancuso, R. J. Comito, R. W. Day, C. H. Hendon, J. T. Miller and M. Dincă, *Chem*, 2018, **4**, 2894–2901.
24 D. J. Xiao, J. Oktawiec, P. J. Milner and J. R. Long, *J. Am. Chem. Soc.*, 2016, **138**, 14371–14379.
25 A. Schaate, P. Roy, A. Godt, J. Lippke, F. Waltz, M. Wiebcke and P. Behrens, *Chem.–Eur. J.*, 2011, **17**, 6643–6651.
26 O. Karagiaridi, W. Bury, J. E. Mondloch, J. T. Hupp and O. K. Farha, *Angew. Chem., Int. Ed.*, 2014, **53**, 4530–4540.
27 Z. Wang and S. M. Cohen, *J. Am. Chem. Soc.*, 2007, **129**, 12368–12369.
28 M. Bui, C. S. Adjiman, A. Bardow, E. J. Anthony, A. Boston, S. Brown, P. S. Fennell, S. Fuss, A. Galindo, L. A. Hackett, J. P. Hallett, H. J. Herzog, G. Jackson, J. Kemper, S. Krevor, G. C. Maitland, M. Matuszewski, I. S. Metcalfe, C. Petit, G. Puxty, J. Reimer, D. M. Reiner, E. S. Rubin, S. A. Scott, N. Shah, B. Smit, J. P. M. Trusler, P. Webley, J. Wilcox and N. Mac Dowell, *Energy Environ. Sci.*, 2018, **11**, 1062–1176.
29 V. M. Krishnamurthy, G. K. Kaufman, A. R. Urbach, I. Gitlin, K. L. Gudiksen, D. B. Weibel and G. M. Whitesides, *Chem. Rev.*, 2008, **108**, 946–1051.
30 K. Sumida, D. L. Rogow, J. A. Mason, T. M. McDonald, E. D. Bloch, Z. R. Herm, T.-H. Bae and J. R. Long, *Chem. Rev.*, 2012, **112**, 724–781.
31 C. A. Trickett, A. Helal, B. A. Al-Maythalony, Z. H. Yamani, K. E. Cordova and O. M. Yaghi, *Nat. Rev. Mater.*, 2017, **2**, 17045.
32 P. C. Sahoo, Y. N. Jang and S. W. Lee, *J. Cryst. Growth*, 2013, **373**, 96–101.
33 P.-Q. Liao, H. Chen, D.-D. Zhou, S.-Y. Liu, C.-T. He, Z. Rui, H. Ji, J.-P. Zhang and X.-M. Chen, *Energy Environ. Sci.*, 2015, **8**, 1011–1016.
34 P. Schmieder, D. Denysenko, M. Grzywa, B. Baumgärtner, I. Senkovska, S. Kaskel, G. Sastre, L. van Wüllen and D. Volkmer, *Dalton Trans.*, 2013, **42**, 10786.
35 D. Denysenko, M. Grzywa, M. Tonigold, B. Streppel, I. Krkljus, M. Hirscher, E. Mugnaioli, U. Kolb, J. Hanss and D. Volkmer, *Chem.–Eur. J.*, 2011, **17**, 1837–1848.
36 S. Biswas, M. Tonigold, M. Speldrich, P. Kögerler, M. Weil and D. Volkmer, *Inorg. Chem.*, 2010, **49**, 7424–7434.
37 C. Jin, S. Zhang, Z. Zhang and Y. Chen, *Inorg. Chem.*, 2018, **57**, 2169–2174.
38 A. Looney, R. Han, K. McNeill and G. Parkin, *J. Am. Chem. Soc.*, 1993, **115**, 4690–4697.
39 H. Schwarz, *Angew. Chem., Int. Ed.*, 2011, **50**, 10096–10115.
40 V. C. C. Wang, S. Maji, P. P. Y. Chen, H. K. Lee, S. S. F. Yu and S. I. Chan, *Chem. Rev.*, 2017, **117**, 8574–8621.
41 R. L. Lieberman and A. C. Rosenzweig, *Nature*, 2005, **434**, 177–182.
42 M. O. Ross, F. MacMillan, J. Wang, A. Nisthal, T. J. Lawton, B. D. Olafson, S. L. Mayo, A. C. Rosenzweig and B. M. Hoffman, *Science*, 2019, **364**, 566–570.
43 A. C. Rosenzweig, C. A. Frederick, S. J. Lippard and P. Nordlund, *Nature*, 1993, **366**, 537–543.
44 T. Ikuno, J. Zheng, A. Vjunov, M. Sanchez-Sanchez, M. A. Ortuño, D. R. Pahls, J. L. Fulton, D. M. Camaioni, Z. Li, D. Ray, B. L. Mehdi, N. D. Browning, O. K. Farha, J. T. Hupp, C. J. Cramer, L. Gagliardi and J. A. Lercher, *J. Am. Chem. Soc.*, 2017, **139**, 10294–10301.
45 J. Zheng, J. Ye, M. A. Ortuño, J. L. Fulton, O. Y. Gutiérrez, D. M. Camaioni, R. K. Motkuri, Z. Li, T. E. Webber, B. L. Mehdi, N. D. Browning, R. L. Penn, O. K. Farha, J. T. Hupp, D. G. Truhlar, C. J. Cramer and J. A. Lercher, *J. Am. Chem. Soc.*, 2019, **141**, 9292–9304.
46 D. Y. Osadchii, A. I. Olivos-Suarez, Á. Szécsényi, G. Li, M. A. Nasalevich, I. A. Dugulan, P. S. Crespo, E. J. M. Hensen, S. L. Veber, M. V. Fedin, G. Sankar, E. A. Pidko and J. Gascon, *ACS Catal.*, 2018, **8**, 5542–5548.
47 R. Balasubramanian, S. M. Smith, S. Rawat, L. A. Yatsunyk, T. L. Stemmler and A. C. Rosenzweig, *Nature*, 2010, **465**, 115–119.
48 K. T. Dinh, M. M. Sullivan, P. Serna, R. J. Meyer, M. Dincă and Y. Román-Leshkov, *ACS Catal.*, 2018, **8**, 8306–8313.
49 K. T. Dinh, M. M. Sullivan, K. Narsimhan, P. Serna, R. J. Meyer, M. Dincă and Y. Román-Leshkov, *J. Am. Chem. Soc.*, 2019, **141**, 11641–11650.
50 B. E. R. Snyder, L. H. Böttger, M. L. Bols, J. J. Yan, H. M. Rhoda, A. B. Jacobs, M. Y. Hu, J. Zhao, E. Ercan Alp, B. Hedman, K. O. Hodgson, R. A. Schoonheydt, B. F. Sels and E. I. Solomon, *Proc. Natl. Acad. Sci. U. S. A.*, 2018, **115**, 4565–4570.
51 M. B. Park, E. D. Park and W.-S. Ahn, *Front. Chem.*, 2019, **7**, 1–7.
52 D. J. Xiao, E. D. Bloch, J. A. Mason, W. L. Queen, M. R. Hudson, N. Planas, J. Borycz, A. L. Dzubak, P. Verma, K. Lee, F. Bonino, V. Crocellà, J. Yano, S. Bordiga, D. G. Truhlar, L. Gagliardi, C. M. Brown and J. R. Long, *Nat. Chem.*, 2014, **6**, 590–595.
53 P. Verma, K. D. Vogiatzis, N. Planas, J. Borycz, D. J. Xiao, J. R. Long, L. Gagliardi and D. G. Truhlar, *J. Am. Chem. Soc.*, 2015, **137**, 5770–5781.
54 E. I. Solomon, K. M. Light, L. V. Liu, M. Srnec and S. D. Wong, *Acc. Chem. Res.*, 2013, **46**, 2725–2739.
55 E. I. Solomon, A. Decker and N. Lehnert, *Proc. Natl. Acad. Sci. U. S. A.*, 2003, **100**, 3589–3594.
56 W. T. Borden, R. Hoffmann, T. Stuyver and B. Chen, *J. Am. Chem. Soc.*, 2017, **139**, 9010–9018.
57 N. Kitajima and Y. Moro-oka, *Chem. Rev.*, 1994, **94**, 737–757.
58 A. J. Jasniewski and L. Que, *Chem. Rev.*, 2018, **118**, 2554–2592.
59 E. D. Bloch, L. J. Murray, W. L. Queen, S. Chavan, S. N. Maximoff, J. P. Bigi, R. Krishna, V. K. Peterson,

F. Grandjean, G. J. Long, B. Smit, S. Bordiga, C. M. Brown and J. R. Long, *J. Am. Chem. Soc.*, 2011, **133**, 14814–14822.
60 J. B. Vincent, G. L. Olivier-Lilley and B. A. Averill, *Chem. Rev.*, 1990, **90**, 1447–1467.
61 D. Denysenko, M. Grzywa, J. Jelic, K. Reuter and D. Volkmer, *Angew. Chem., Int. Ed.*, 2014, **53**, 5832–5836.
62 M. P. Lanci, V. V. Smirnov, C. J. Cramer, E. V. Gauchenova, J. Sundermeyer and J. P. Roth, *J. Am. Chem. Soc.*, 2007, **129**, 14697–14709.
63 C. E. Elwell, N. L. Gagnon, B. D. Neisen, D. Dhar, A. D. Spaeth, G. M. Yee and W. B. Tolman, *Chem. Rev.*, 2017, **117**, 2059–2107.
64 I. M. Wasser, S. de Vries, P. Moënne-Loccoz, I. Schröder and K. D. Karlin, *Chem. Rev.*, 2002, **102**, 1201–1234.
65 L. K. Keefer, *Nat. Mater.*, 2003, **2**, 357–358.
66 B. Xiao, P. S. Wheatley, X. Zhao, A. J. Fletcher, S. Fox, A. G. Rossi, I. L. Megson, S. Bordiga, L. Regli, K. M. Thomas and R. E. Morris, *J. Am. Chem. Soc.*, 2007, **129**, 1203–1209.
67 A. C. McKinlay, B. Xiao, D. S. Wragg, P. S. Wheatley, I. L. Megson, R. E. Morris, A. C. McKinlay, B. Xiao, D. S. Wragg, P. S. Wheatley, I. L. Megson and R. E. Morris, *J. Am. Chem. Soc.*, 2008, **130**, 10440–10444.
68 F. Bonino, S. Chavan, J. G. Vitillo, E. Groppo, G. Agostini, C. Lamberti, P. D. C. Dietzel, C. Prestipino and S. Bordiga, *Chem. Mater.*, 2008, **20**, 4957–4968.
69 A. C. McKinlay, J. F. Eubank, S. Wuttke, B. Xiao, P. S. Wheatley, P. Bazin, J.-C. Lavalley, M. Daturi, A. Vimont, G. De Weireld, P. Horcajada, C. Serre and R. E. Morris, *Chem. Mater.*, 2013, **25**, 1592–1599.
70 E. D. Bloch, W. L. Queen, S. Chavan, P. S. Wheatley, J. M. Zadrozny, R. Morris, C. M. Brown, C. Lamberti, S. Bordiga and J. R. Long, *J. Am. Chem. Soc.*, 2015, **137**, 3466–3469.
71 K. Peikert, L. J. McCormick, D. Cattaneo, M. J. Duncan, F. Hoffmann, A. H. Khan, M. Bertmer, R. E. Morris and M. Fröba, *Microporous Mesoporous Mater.*, 2015, **216**, 118–126.
72 D. Cattaneo, S. J. Warrender, M. J. Duncan, C. J. Kelsall, M. K. Doherty, P. D. Whitfield, I. L. Megson and R. E. Morris, *RSC Adv.*, 2016, **6**, 14059–14067.
73 R. R. Haikal, C. Hua, J. J. Perry, D. O'Nolan, I. Syed, A. Kumar, A. H. Chester, M. J. Zaworotko, M. H. Yacoub and M. H. Alkordi, *ACS Appl. Mater. Interfaces*, 2017, **9**, 43520–43528.
74 C. K. Brozek, J. T. Miller, S. A. Stoian and M. Dincă, *J. Am. Chem. Soc.*, 2015, **137**, 7495–7501.
75 J. Jover, C. K. Brozek, M. Dincă and N. López, *Chem. Mater.*, 2019, **31**, 8875–8885.
76 A. J. Rieth, A. M. Wright and M. Dincă, *Nat. Rev. Mater.*, 2019, **4**, 708–725.